

RESEARCH PAPER

 OPEN ACCESS 

## Danshensu alleviates bleomycin-induced pulmonary fibrosis by inhibiting lung fibroblast-to-myofibroblast transition via the MEK/ERK signaling pathway

Huaman Liu<sup>a,b</sup>, Xinyue Zhang<sup>c</sup>, Yumeng Shao<sup>a</sup>, Xuehong Lin<sup>b</sup>, Feng Dong<sup>b</sup>, and Xue Liu<sup>c,d\*</sup>

<sup>a</sup>College of Traditional Chinese Medicine, Shandong University of Traditional Chinese Medicine, Jinan, China; <sup>b</sup>Department of General Medicine, The Affiliated Hospital of Shandong University of Traditional Chinese Medicine, Jinan, China; <sup>c</sup>First College of Clinical Medicine, Shandong University of Traditional Chinese Medicine, Jinan, China; <sup>d</sup>Department of Respiration, The Affiliated Hospital of Shandong University of Traditional Chinese Medicine, Jinan, China

### ABSTRACT

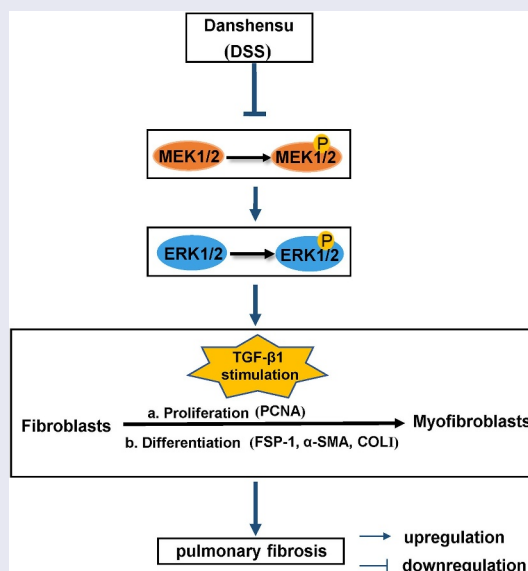
Pulmonary fibrosis (PF) is a chronic pulmonary interstitial disease, and its pathological process is closely related to fibroblast–myofibroblast differentiation. Danshensu (DSS) has been reported to exert an anti-fibrotic effect in heart and liver. However, it is unknown whether DSS has an equally anti-fibrotic effect on lungs. To evaluate the effect of DSS on PF and demonstrate its possible molecular mechanisms, we established an *in vitro* model on TGF- $\beta$ 1 (5 ng/mL)-stimulated NIH3T3 cells and *in vivo* model on bleomycin (BLM) (5 mg/kg)-induced PF mice. *In vitro*, our results revealed that 50  $\mu$ M DSS effectively inhibited the fibroblast proliferation, migration and differentiation into myofibroblast. *In vivo*, our results showed that DSS (28 and 56 mg/kg) reduced damaged lung structures, infiltrated inflammatory cells and accumulated areas of collagen deposition. Moreover, we showed that DSS decreased the fibroblast-specific protein 1 (FSP-1) – and  $\alpha$ -SMA-positive areas. Meanwhile, we indicated that DSS reduced the expression of TGF- $\beta$ 1,  $\alpha$ -SMA and COL-I in the lung tissues of mice. To further explore the mechanism of DSS on alleviating PF, we detected the MEK/ERK signaling pathway. Our results showed that DSS reduced the phosphorylation of MEK1/2 and ERK1/2, indicating that DSS might inhibit the MEK/ERK signaling pathway. Taken together, these results demonstrated that DSS could suppress lung fibroblast proliferation, migration and differentiation to myofibroblasts, possibly through suppressing the MEK/ERK signaling pathway, which suggested that DSS might be a potential therapeutic drug for PF treatment.

### ARTICLE HISTORY

Received 8 April 2021  
Revised 11 June 2021  
Accepted 12 June 2021

### KEYWORDS

Pulmonary fibrosis;  
danshensu; fibroblast;  
myofibroblasts; MEK; ERK



\*CONTACT Dr. Xue Liu  [liuxue52055@126.com](mailto:liuxue52055@126.com)  Department of Respiration, The Affiliated Hospital of Shandong University of Traditional Chinese Medicine, No. 16369, Jingshi Road, Jinan, 250014, China; First College of Clinical Medicine, Shandong University of Traditional Chinese Medicine, No. 4655, Daxue Road, Jinan 250355, China.

© 2021 The Author(s). Published by Informa UK Limited, trading as Taylor & Francis Group.  
This is an Open Access article distributed under the terms of the Creative Commons Attribution License (<http://creativecommons.org/licenses/by/4.0/>), which permits unrestricted use, distribution, and reproduction in any medium, provided the original work is properly cited.

## Introduction

Pulmonary fibrosis (PF), as a chronic pulmonary interstitial disease, is characterized by aberrant fibroblast proliferation, excessive extracellular matrix (ECM) accumulation, inflammatory damage and tissue structure destruction, which ultimately leads to lung scarring formation, pulmonary insufficiency and respiratory failure [1,2]. PF has high mortality and poor prognosis with unknown causes [3,4]. Several explanations including oxidative stress [5], inflammatory response [6,7], fibroblast activation and abnormal deposition of ECM [8] have been involved in the pathogenesis of PF. Importantly, the progression of fibroblasts differentiating into myofibroblasts is likely the key to PF [4]. Under the stimulation of pathological factors such as TGF- $\beta$ 1<sup>8</sup>, fibroblasts can proliferate and differentiate into  $\alpha$ -smooth muscle actin ( $\alpha$ -SMA)-positive myofibroblasts in large numbers [9,10]. These myofibroblasts acquire an aggressive phenotype followed by the accumulation of type collagen, abnormal deposition of ECM and acceleration of PF remodeling [11,12]. Therefore, to explore new ways for alleviating PF is of great significance.

Danshensu (DSS), one of the main active ingredients in Danshen, has various pharmacological activities such as anti-apoptosis, anti-oxidation, and anti-inflammation [13]. Particularly, Luo et al. have found that *Salvia miltiorrhiza* Bunge (containing DSS) can relieve inflammation and airway remodeling in asthma model mice, and inhibit TGF- $\beta$ 1-induced epithelial-mesenchymal transition (EMT) and fibrosis in BEAS-2B and MRC-5 cells [14]. Moreover, several studies have shown that DSS can improve liver fibrosis and myocardial fibrosis by inhibiting oxidative stress response [15,16]. Hence, we hypothesized that DSS might attenuate PF via inhibiting fibroblast-myofibroblast differentiation.

To explore the role of DSS in PF, we first established an *in vitro* model on TGF- $\beta$ 1 (5 ng/mL)-stimulated NIH3T3 cells and determined the function of DSS on the fibroblast proliferation, migration and differentiation into myofibroblast. Furthermore, we performed an *in vivo* model on bleomycin (BLM)

(5 mg/kg)-induced PF mice to evaluate the effect of DSS on lung structures and collagen deposition. Finally, western blot assay was used to detect the MEK/ERK signaling pathway.

## Materials and methods

### Cell culture

DSS (purity >98%; molecular weight 198.17), purchased from Meilunbio (Dalian, China), was dissolved in sterile distilled water as a 40-mM stock solution. NIH3T3 cells (Procell Life Science & Technology Co., Ltd., Wuhan, China) were cultured in Dulbecco's modified eagle medium (DMEM, Gibco, USA) containing 10% fetal bovine serum (FBS) in a 37°C, 5% CO<sub>2</sub> incubator. Then, NIH3T3 cells were treated in different ways as followed: part of NIH3T3 cells were treated with DSS at different concentrations (0, 25, 50, 100, 200, and 400  $\mu$ M) for 24 h; part of NIH3T3 cells were pretreated with various concentrations of DSS (0, 25, 50, 100, 200, and 400  $\mu$ M) for 2 h, followed by stimulation with or without TGF- $\beta$ 1 (5 ng/mL) for 24 h and another part of NIH3T3 cells were pretreated with DSS (50  $\mu$ M) for 2 h, followed by the stimulation with or without TGF- $\beta$ 1 (5 ng/mL) for 24 h.

### Cell Counting Kit-8 (CCK-8) assay

The CCK-8 kit (KGA317, Keygenbio, Nanjing, China) was used to assess cell viability and cell proliferation. NIH3T3 cells were seeded in 96-well plates at a density of  $5 \times 10^3$  cells per well. After NIH3T3 cells were treated, the CCK-8 solution (10  $\mu$ L) was added to each well and incubated at 37°C for 2 h. The optical density was read at a wavelength of 450 nm with microplate reader (800Ts, BIOTEK, USA).

### Wound healing assay

NIH3T3 cells were seeded in 6-well plates. When the cell density reached about 90%, the medium was replaced with serum-free medium and treated with 1  $\mu$ g/mL mitomycin C (M0503, Sigma-Aldrich, USA) for 1 h. Then, a 200  $\mu$ L pipette tip was used to scratch the cells. The wounded gaps

were photographed at 0 h and 24 h under a microscope at a magnification of 100× (DP73, OLYMPUS, Japan) and the wound healing ratio of each group was calculated.

### **Quantitative real-time PCR (qRT-PCR)**

Total RNA was isolated from NIH3T3 cells by using Total RNA fast extraction kit (RP1202, BioTeke, China) following the manufacturer's protocol. RNA concentration was determined using the UV spectrophotometer NANO 2000 (Thermo, USA). The RNAs were reverse transcribed into cDNAs, which was performed by using Super M-MLV Reverse Transcriptase (BioTeke) according to the manufacturer's instructions. Real-time PCR was performed in 20 µL reactions on cDNA with SYBR Green (EP1602, BioTeke) and Taq HS Perfect Mix (R300A, Takara, Japan) by using Exicycler™ 96 Real-time Quantitative Thermal Block (BIONEER, Korea). The level of target mRNA was normalized to the level of GAPDH. Data were analyzed with a  $2^{-\Delta\Delta CT}$  method. Each gene analysis was performed in triplicate. Primer sequences of the targeted genes were listed as followed: Colla1 forward: CGCCATCAAGGTCTACTGC, Colla1 reverse: GAATCCATCGGTCATGCTCT;  $\alpha$ -SMA forward: GACGCTGAAGTATCCGATAGAACACG,  $\alpha$ -SMA reverse: CACCATCTCCAGAGTCCAGCACAAT; GAPDH forward: TGTTCCTACCCCAATGTGTCCGTC, GAPDH reverse: CTGGTCCTCAGTGTAGCCCAAGATG.

### **Immunofluorescence staining**

NIH3T3 cells were first fixed with 4% formaldehyde for 15 min at room temperature (RT). After treated with 0.1% Triton X-100 (ST795, Beyotime, China) for 30 min at RT, NIH3T3 cells were blocked with goat serum (SL038, Solarbio, China) at RT for 15 min followed by an incubation with the primary antibody against  $\alpha$ -SMA (1:200; AF1032, Affinity, China)

overnight at 4°C. Next, the cells were incubated with Cy3-labeled goat anti-rabbit IgG (1:200, A0516, Affinity) for 1 h at RT. DAPI was used to counter-stain cell nuclei for 5 min at 37°C, and the cells were photographed under a microscope at a magnification of 400 × .

### **Animals**

C57BL/6 male mice aged 7–8 weeks were purchased from Liaoning Changsheng biotechnology co., Ltd (Liaoning, China). All mice were maintained under standard conditions at our animal facility (temperature of  $22 \pm 1^\circ\text{C}$ , humidity of 45–55% and a 12-h light/dark cycle) with a specific pathogen-free environment, free access to food and water. All animal experiments were approved by the Animal Research Ethics Board of The Affiliated Hospital of Shandong University (Permission Number: 2019–58), in accord with the Guide for the Care and Use of Laboratory Animals.

### **Establishment of PF induced by BLM in mice**

The experiment of BLM-induced PF in mice was performed as previously reported [17]. Briefly, after a week of adaptive feeding, C57BL/6 mice were divided randomly into four groups: (1) the control group; (2) the BLM group; (3) BLM + DSS (28 mg/kg) group; (4) BLM + DSS (56 mg/kg) group. A single intratracheal instillation of BLM (5 mg/kg) was performed to induce PF in mice. Mice in the control group received an equal volume of saline. One day after BLM treatment, mice in the BLM + DSS group were intragastrically administration of DSS (28 mg/kg or 56 mg/kg) while mice in BLM group were intragastrically administrated with equal volume 0.9% sterilized saline. After 3 weeks, mice were sacrificed and lung tissues were collected and measured. The pulmonary index was calculated using the following formula: Pulmonary index = (Lung weight (mg)) / (Body weight (g)) × 100%.

### **Hematoxylin-eosin (HE) and sirusred staining**

The lung tissues were fixed with 4% paraformaldehyde, dehydrated in 70% (2 h), 80% (overnight),

90% (2 h), 100% I (1 h), 100% II (1 h) gradient alcohol, permeabilized in xylene for 30 min, embedded in paraffin, and cut into 5- $\mu$ m slices for subsequent experiments. After deparaffinization and hydration, the slices were heated with the antigen retrieval solution for 10 min. Then, the slices were stained with hematoxylin and eosin (WLA051a, Wanleibio, China) and sirusred (S8060, Solarbio, China) respectively. Finally, the slices were mounted for observation under a microscope.

### Immunohistochemistry (IHC)

IHC was performed to evaluate the fibrotic phenotype of lung tissues. After deparaffinization and hydration, the slices were heated with the antigen retrieval solution for 10 min. Then, the slices were penetrated with PBS for 5 min followed with H<sub>2</sub>O<sub>2</sub> treatment for about 15 min, and then blocked with goat serum (SL038, Solarbio) for 60 min at RT to eliminate the activity of endogenous peroxidase. The slices were incubated overnight at 4°C with antibodies against the following proteins:  $\alpha$ -SMA (1:200, AF1032, Affinity) and fibroblast-specific protein 1 (FSP-1, 1: 200, A19109, Abclonal). The next day, the slices were incubated with HRP-labeled secondary antibody (1:500, #31460, ThermoFisher, USA) at 37°C for 60 min. After developed with DAB reagent (DA1010, Solarbio), the slices were then counterstained with hematoxylin (H8070, Solarbio). Finally, the slides were mounted and observed under a microscope.

### Western blot

Proteins were extracted by mixing RIPA lysate (R0010, Solarbio) and PMSF (P0100, Solarbio). The concentrations of proteins were assayed by the BCA kit (PC0020, Solarbio). According to different molecular weights, 5% concentrated gel and 8% separation gel concentrations were used in the SDS-PAGE. After transferred to a PVDF membrane, the proteins were blocked by prepared 5% (M/V) BSA (Biosharp, BS043, China) in TBST buffer for 1 h and incubated overnight at 4 °C with the following primary antibodies:  $\alpha$ -SMA (1: 500), COL-I (1: 500, AF0134, Affinity), TGF- $\beta$ 1 (1: 1000, AF1027,

Affinity), proliferating cell nuclear antigen (PCNA) (1: 500, A12427, Abclonal, China), p-MEK1/2 (1: 500, AP0209, Abclonal), MEK1/2 (1: 500, A4868, Abclonal), p-ERK1/2 (1: 500, AF1015, Affinity), ERK1/2 (1: 500, AF6240, Affinity) and GAPDH (1: 10000, 60004-1-Ig, Proteintech, China). Next, the membrane was incubated with goat anti-mouse IgG (1: 3000, SE131, Solarbio) or goat anti-rabbit IgG (1: 3000, SE134, Solarbio) secondary antibody for 40 min at 37 °C. At last, the specific protein bands were visualized with Western ECL Substrate (D1010, Solarbio).

### Statistical analysis

Data were expressed as mean  $\pm$  standard deviation (SD). Statistical significance was assessed by one-way analysis of variance (ANOVA).  $P < 0.05$  was considered statistically significant.

### Results

To explore the function and mechanism of DSS in PF, we established an *in vitro* model on TGF- $\beta$ 1 (5 ng/mL)-stimulated NIH3T3 cells and an *in vivo* model on bleomycin (BLM) (5 mg/kg)-induced PF mice. Functionally, we determined the fibroblast proliferation, migration and differentiation into myofibroblast *in vitro*. Moreover, we evaluated the effect of DSS on lung structures and collagen deposition *in vivo*. Mechanically, western blot assay was used to detect the MEK/ERK signaling pathway.

#### Effects of DSS on the migration and proliferation of NIH3T3 cells

CCK-8 assay was used to select the appropriate concentration of DSS for subsequent experiments. Our results showed that compared with the control cells, there was no significant difference in the effects of 25  $\mu$ M and 50  $\mu$ M DSS on cell viability (Figure 1a). Besides, 50  $\mu$ M DSS had a better effect on reducing cell proliferation induced by TGF- $\beta$ 1 (Figure 1b). Hence, 50  $\mu$ M DSS was selected for subsequent experiments. To further verify the role of DSS in the migration and proliferation of TGF- $\beta$ 1-induced

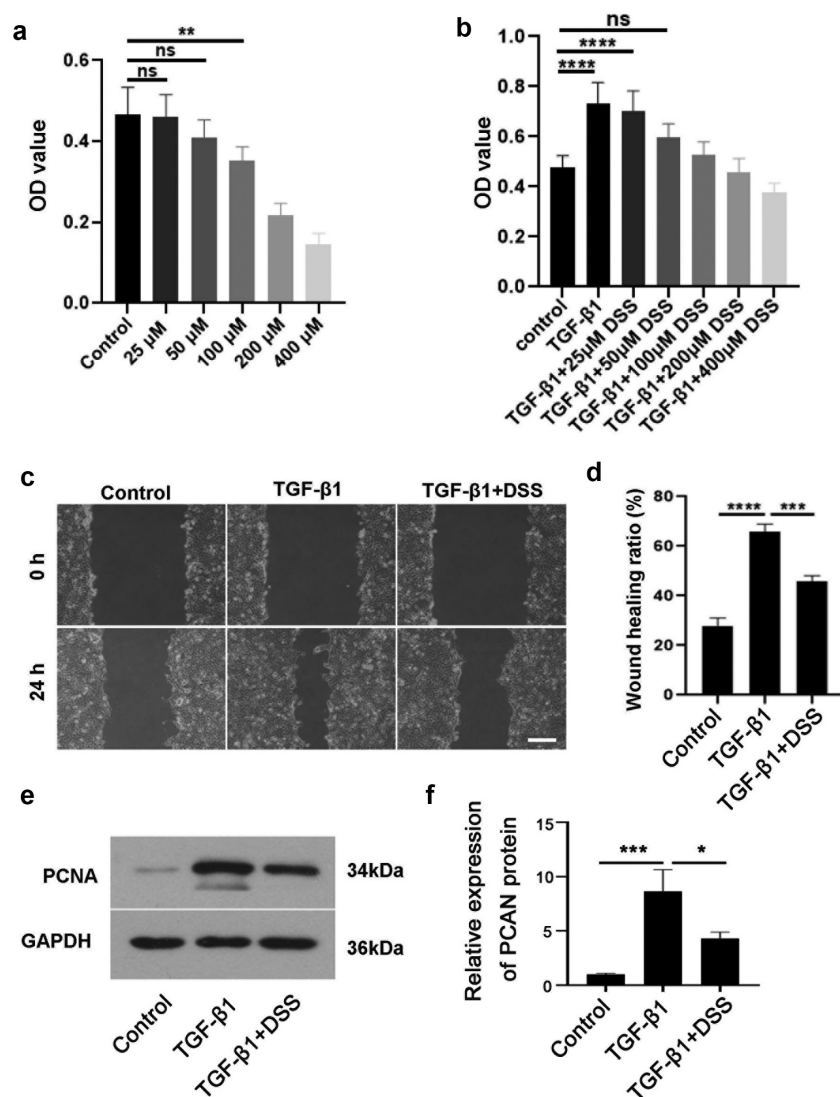


**Figure 1.** DSS repressed the proliferation and migration of NIH3T3 cells induced by TGF- $\beta$ 1. NIH3T3 cells were treated with TGF- $\beta$ 1 (5 ng/mL) in the absence or presence of DSS for 24 h. (a) The effect of DSS (25, 50, 100, 200 and 400  $\mu$ M) on the cell viability was detected by CCK-8 assay. (b) The effect of DSS (25, 50, 100, 200 and 400  $\mu$ M) on the cell viability induced by TGF- $\beta$ 1 was detected by CCK-8 assay. (c) Effects of DSS (50  $\mu$ M) on the cell migration were detected by wound healing analysis. Scale bar: 200  $\mu$ m. (d) The calculation of wound healing ratio. (e, f) The expression of PCNA was detected by western blot assay. GAPDH was conducted as a loading control. One-way ANOVA, \* $p < 0.05$ , \*\* $p < 0.01$ , \*\*\* $p < 0.001$ , \*\*\*\* $p < 0.0001$ , ns: non-significant.

NIH3T3 cells, we performed wound healing assay and detected the expression of proliferation-related protein PCNA. Our results showed that DSS significantly reduced the migration of NIH3T3 cells induced by TGF- $\beta$ 1 (Figure 1c and Figure 1d) ( $p < 0.01$ ). Western blot result indicated that TGF- $\beta$ 1 promoted PCNA expression, while DSS reversed this result (Figure 1e and Figure 1f). Collectively, these results revealed that DSS suppressed the migration

and proliferation in TGF- $\beta$ 1-induced NIH3T3 cells.

#### **Effects of DSS on fibroblast-myofibroblast differentiation and the MEK/ERK signaling pathway in TGF- $\beta$ 1-induced NIH3T3 cells**

COL-I and  $\alpha$ -SMA are markers of fibroblast differentiation to myofibroblasts [18]. Hence, to establish if DSS inhibited TGF- $\beta$ 1-induced

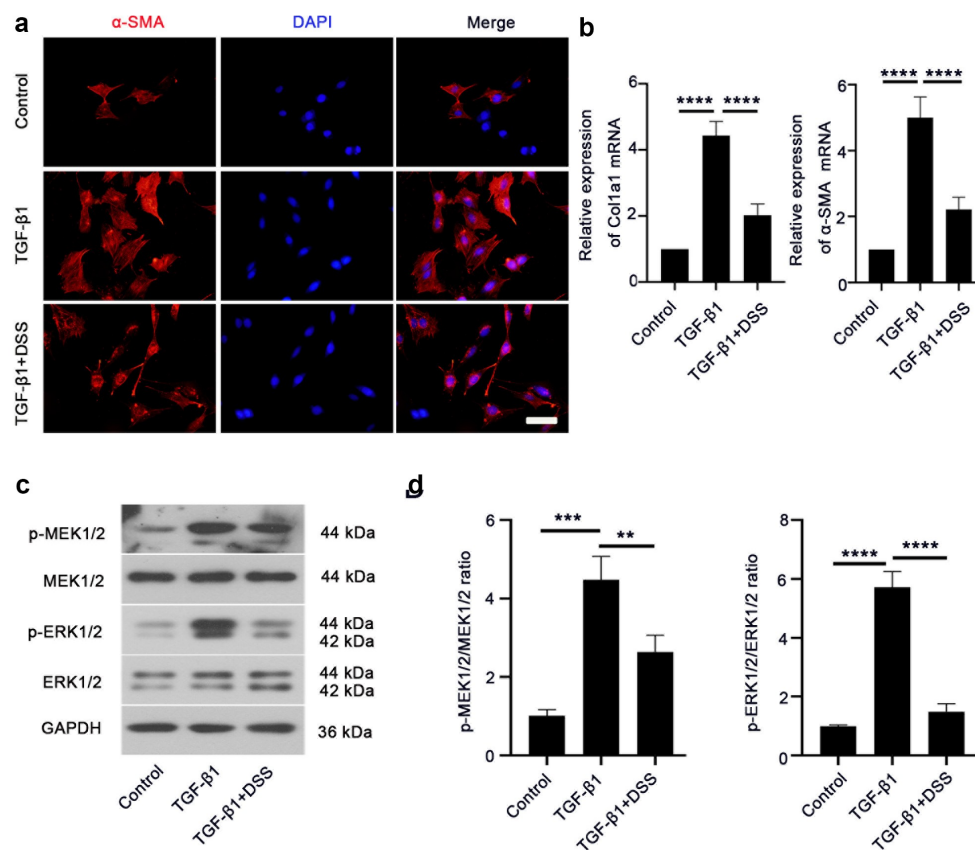


**Figure 2.** DSS inhibited TGF- $\beta$ 1-induced fibroblast-myofibroblast differentiation via inhibiting the MEK/ERK signaling pathway in NIH3T3 cells. (a) Immunofluorescence was conducted to evaluate the expression of  $\alpha$ -SMA (red). Nucleus was stained with DAPI (blue). Scale bar: 50  $\mu$ m. (b) Relative mRNA expression of Col1a1 and  $\alpha$ -SMA. (c, d) Expressions of p-MEK1/2, MEK1/2, p-ERK1/2, ERK1/2 were detected by western blot. GAPDH was conducted as a loading control. One-way ANOVA, \*\* $p < 0.01$ , \*\*\* $p < 0.001$ , \*\*\*\* $p < 0.0001$ .

fibroblast-myofibroblast differentiation, the expression of  $\alpha$ -SMA and COL-I was assessed. Immunofluorescence staining result showed that  $\alpha$ -SMA expression after DSS treatment was weaker than that in the TGF- $\beta$ 1-treated cells (Figure 2a). The mRNA level of Col1a1 and  $\alpha$ -SMA was significantly reduced by DSS administration compared with the TGF- $\beta$ 1-treated cells (Figure 2b). To further explore the mechanism of DSS on inhibiting fibroblast-myofibroblast differentiation, we evaluated the potential role of the MEK/ERK signaling pathway. Western blot assay exhibited that TGF- $\beta$ 1 elevated the expression of MEK1/2 and ERK1/2 phosphorylation. After DSS treatment, the phosphorylation of MEK1/2 and ERK1/2 was decreased (Figure 2c and Figure 2d). These results suggested that DSS might suppress fibroblast-myofibroblast differentiation via

inhibiting the MEK/ERK signaling pathway in TGF- $\beta$ 1-induced NIH3T3 cells.

### Effects of DSS on BLM-induced fibrotic lesions in the lung of mice

To further examine the effect of DSS *in vivo*, BLM-induced PF model was used. After treated with BLM alone, damaged lung structures, thickened alveolar walls, infiltrated inflammatory cells and accumulated areas of collagen deposition were observed in the lung tissues of mice. However, DSS administration alleviated the results induced by BLM (Figure 3a and Figure 3b). Histological scores analysis indicated that DSS reduced the severity of PF (Figure 3c). Moreover, decreased pulmonary index was found with DSS treatment compared with BLM treatment alone (Figure 3d). Hence,

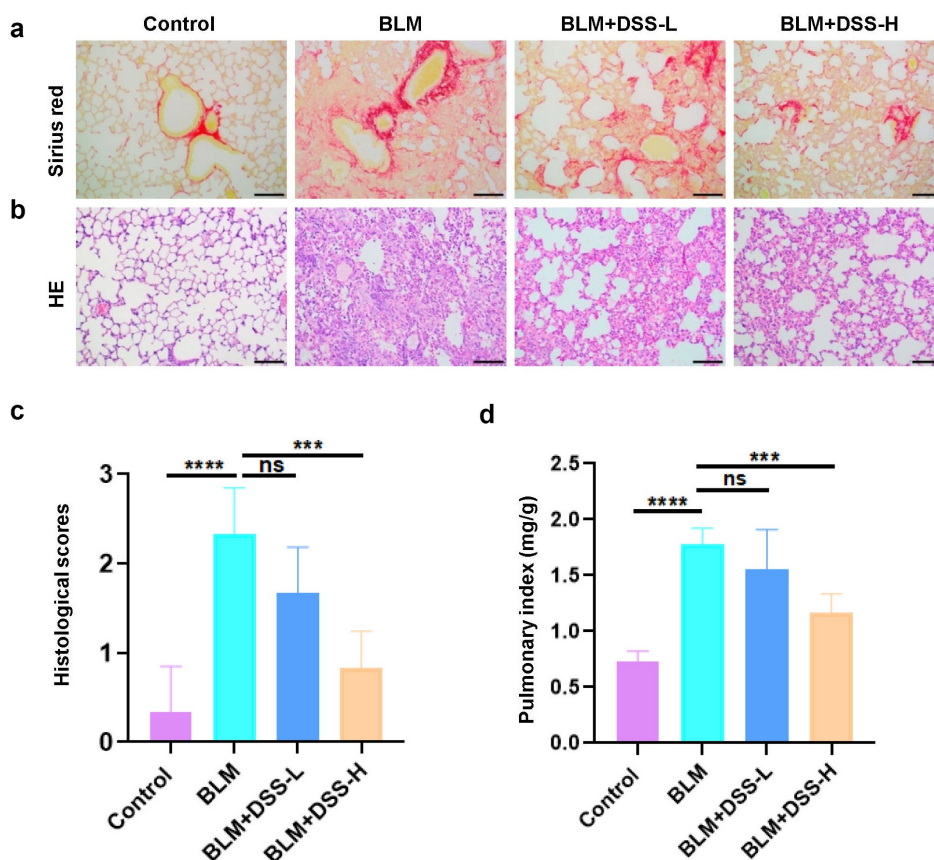


**Figure 3.** DSS alleviated BLM-induced PF in mice. (a-b) Sections of lung tissue were stained with HE staining and sirius red staining. Scale bar: 100  $\mu$ m. (c) Histological scores. (d) The pulmonary index was measured. One-way ANOVA, \*\*\* $p < 0.001$ , \*\*\*\* $p < 0.0001$ , ns: non-significant.

these data exhibited that DSS alleviated BLM-induced fibrotic lesions in the lung of mice.

#### Effects of DSS on fibroblast-myofibroblast differentiation in BLM-induced mice

To assess whether DSS inhibited fibroblast-myofibroblast differentiation in BLM-induced mice, we investigated the expression of FSP-1,  $\alpha$ -SMA and COL-I. FSP-1 – and  $\alpha$ -SMA-positive areas were obviously increased in lungs of BLM-treated mice, while DSS (28 and 56 mg/kg) decreased the FSP-1 – and  $\alpha$ -SMA-positive areas (Figure 4a). Additionally, western blot results showed that treatment with BLM resulted in an increase in the expression of  $\alpha$ -SMA and COL-I in the lung tissues of mice, while DSS reversed the results (Figure 4b and Figure 4c). Meanwhile, decreased protein level

of TGF- $\beta$ 1 was observed in DSS-treated mice compared with BLM group (Figure 4b and Figure 4c). Furthermore, we detected the MEK/ERK signaling pathway. In line with *in vitro* results, we found that DSS repressed the phosphorylation of MEK1/2 and ERK1/2 in BLM-treated mice (Figure 4d and Figure 4e). Taken together, these results indicated that DSS inhibited the fibroblast-myofibroblast differentiation via inhibiting the MEK/ERK signaling pathway in BLM-induced mice.

#### Discussion

PF is a progressive disease, which can lead to death. With PF onset, fibroblasts will proliferate, migrate and differentiate into myofibroblasts to form fibroblast foci [19]. Although pirfenidone and nintedanib have been used clinically to treat

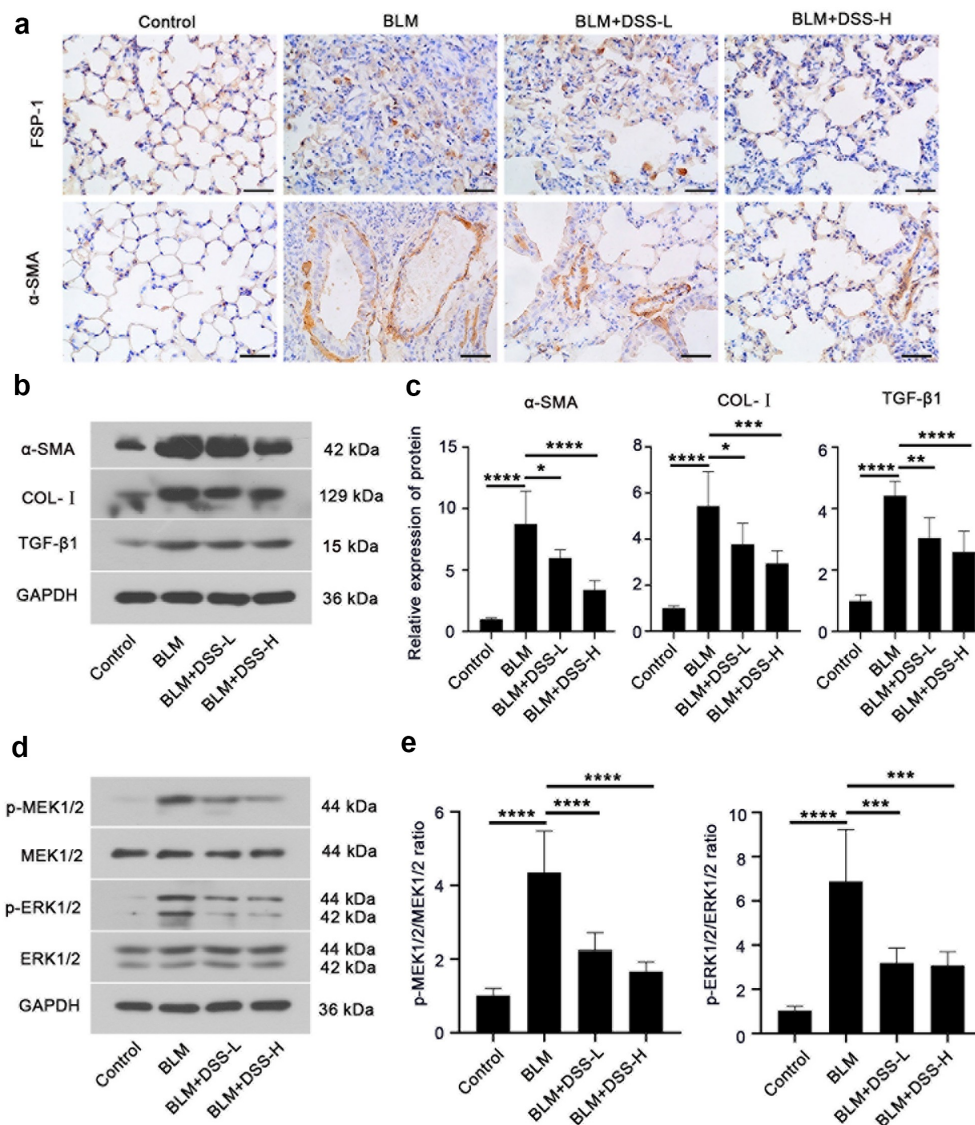


**Figure 4.** DSS inhibited fibroblast-myofibroblast differentiation via inhibiting the MEK/ERK signaling pathway in BLM-induced mice. (a) Immunohistochemistry analysis of FSP-1 and  $\alpha$ -SMA in sections of lung tissues. Scale bar: 50  $\mu$ m. (b, c) Protein expressions of  $\alpha$ -SMA, COL-I, and TGF- $\beta$ 1 were detected by western blot. GAPDH was conducted as a loading control. (d, e) Protein expressions of p-MEK1/2, MEK1/2, p-ERK1/2, ERK1/2 were examined by western blot. GAPDH was conducted as a loading control. One-way ANOVA, \* $p < 0.05$ , \*\*\* $p < 0.001$ , \*\*\*\* $p < 0.0001$ .

PF, none of these can significantly reduce the mortality of patients [20,21]. In addition, there are few effective drugs that can reverse human PF and prevent chronic development of respiratory failure [22]. Therefore, it is a concern to find new effective and targeted therapies for PF. In this study, we found both *in vitro* and *in vivo* that DSS could inhibit fibroblast proliferation, migration, and differentiation into myofibroblast, likely by repressing the MEK/ERK signaling pathway.

First, we found that DSS significantly improved the cell proliferation caused by TGF- $\beta$ 1 with no

effect on cell viability. Meanwhile, we found that DSS inhibited the expression of PCNA, which further confirmed the ability of DSS to inhibit cell proliferation. Consistent with our results, several studies have shown the inhibitory effect of DSS on cell proliferation. For example, Jia et al. has shown that DSS inhibited unusual epidermal proliferation in psoriasis [23]. Zhang et al. has exhibited that DSS can inhibit the proliferation of HSC-T6 in liver fibrosis [24]. Another study has demonstrated that DSS prevents hypoxic pulmonary hypertension in rats by inhibiting the

proliferation of pulmonary artery smooth muscle cells in a TGF- $\beta$ -smad3-associated manner [25]. Interestingly, a research has shown that DSS can promote cell proliferation in Detroit 551 human normal fibroblast cells [26], which does not seem to be consistent with our results. We think it may be due to different cells that DSS acts on, and different ways that cells are treated. There may be interactions in this pathological microenvironment, and the regulation mechanism needs to be further explored. Our study showed that DSS inhibited cell proliferation, which implies that DSS has another side in affecting cell proliferation. Therefore, how to reasonably use DSS to achieve the desired therapeutic effect requires more in-depth research in future clinical applications. Then, we found that DSS could inhibit fibroblast-myofibroblast differentiation by reducing the expression of myofibroblast markers  $\alpha$ -SMA and COL-I. Additionally, we also found that DSS reduced the expression of the prototypical fibroblast marker FSP-1. Similar with our results, Ji et al. has found that Paeoniflorin inhibited PF stimulated by TGF- $\beta$ 1 through suppressing the expression of FSP-1, COL-I and  $\alpha$ -SMA in A549 cells [27]. Vu et al. has shown that interferon- $\gamma$  prevented IPF via down-regulating the expression of COL-I and  $\alpha$ -SMA [18]. Wang et al. has clarified that Fus down-regulated the expression of COL-I and  $\alpha$ -SMA in AngII-induced cardiac fibroblasts [28]. Yang et al. has exhibited that INHBA-S1 silencing alleviated the production of COL-I and  $\alpha$ -SMA by targeting miR-141-3p in human hypertrophic scar fibroblasts [29]. Interestingly, several studies have also shown that DSS plays an important role in other diseases such as cardiac fibrosis [30] and liver fibrosis [24]. Moreover, Shao et al. has revealed the effect of two Chinese herbal medicines containing Danshen on anti-pulmonary fibrosis [31]. Lu et al. has shown that DSS suppresses cardiac fibrosis induced by  $\beta$ -adrenergic receptor via negatively regulating ROS-p38 MAPK signaling [16]. Collectively, these results have suggested that DSS has a potential anti-fibrotic effect.

Furthermore, we detected the expression of TGF- $\beta$ 1 in lungs of BLM-induced mice. TGF- $\beta$ 1 is a key driving force of PF [32]. First, TGF- $\beta$ 1 can promote the accumulation of

collagen, which is beneficial for organ wound repair. However, too frequent ECM reinforcement with collagen as the main component will turn into progressive fibrosis [33]. Studies in cultured epithelial cells and mesenchymal cells have found that TGF- $\beta$ 1 promotes the production of fibronectin and collagen by regulating the transcriptional activation of related genes [34]. In addition, subcutaneous injection of TGF- $\beta$ 1 is believed to strongly promote collagen accumulation and fibrotic tissue response [35]. Second, TGF- $\beta$ 1 is also involved in inflammation regulation [36,37]. A study has reported that deletion of the TGF- $\beta$ 1 gene in mice will cause the mice to die quickly after birth, which is caused by systemic inflammation [37]. Hence, TGF- $\beta$ 1 is generally considered an inhibitor of excessive inflammation [38]. Regulated inflammation plays an important factor in determining tissue repair, limiting the formation of fibrosis by promoting the decomposition of ECM and inhibiting the accumulation of collagen [33,39,40]. However, TGF- $\beta$ 1 can stimulate fibroblasts to produce ECM and inhibit ECM degradation by matrix metalloproteinases [41]. Last but not most important, TGF- $\beta$ 1 can promote the differentiation of fibroblasts into myofibroblasts [42]. A study has shown that the production of myofibroblasts and PF can be observed by transferring the TGF- $\beta$ 1 gene into mouse lung tissue [43]. Zhang et al. has demonstrated that DSS improves pulmonary hypertension by inhibiting TGF- $\beta$ /Smad3 pathway [25]. In our study, we found DSS treatment (28 and 56 mg/kg) reduced TGF- $\beta$ 1 expression in BLM-induced mice, which further confirmed that DSS could alleviate PF. In line with our study, Liu et al. has indicated that DSS repressed the expression of TGF- $\beta$  induced by hypoxia on pulmonary hypertension [44]. It is worth noting that we referred to the DSS concentration used in the existing literature [15,45] and then used the body surface area (BSA) normalization method [46] to calculate the concentration of DSS used in our experiments.

Additionally, TGF- $\beta$ 1 and its downstream effector IL-11 have been reported to activate the MEK/ERK signaling pathway to mediate senescence-associated PF [47]. Hence, to further explore the

molecular mechanism of DSS on alleviating PF, we detected the expression of the MEK/ERK signaling pathway. The MEK/ERK signaling pathway has been involved in the regulation of pulmonary fibrosis [48]. Moreover, Madala, Satish K et al. have shown that using MEK inhibitor ARRY-142,886 (ARRY) to treat lung fibrosis model mice can prevent lung cell proliferation and increase in total lung collagen, and protect mice from changes in lung function, indicating that MEK/ERK activation plays an important role in human PF [49]. Additionally, recent studies have exhibited the inhibitory effect of DSS on the MEK/ERK signaling pathway in cardiovascular diseases [50,51]. In our study, we found that DSS could reduce the expression of p-MEK1/2 and p-ERK1/2, which indicated that DSS might alleviate PF via inhibiting the MEK/ERK signaling pathway.

## Conclusion

Taken together, our research has proposed that DSS can alleviate TGF- $\beta$ 1 – and BLM-induced PF via inhibiting the conversion of fibroblasts to myofibroblasts, possibly through suppressing the MEK/ERK signaling pathway. Our study provides a new sight for the future PF treatment.

## Author Contributions

Liu HM and Liu X constructed the conception. Liu HM, Zhang XY, Shao YM and Liu X searched the literature and conducted the experiments. Shao YM, Lin XH and Dong F analyzed the data. Liu HM and Liu X wrote the manuscript. All authors read and approved the manuscript.

## Disclosure of potential conflicts of interest

No potential conflict of interest was reported by the author(s).

## Funding

This work was supported by the the National Nature Science Foundation of China [81804034].

## Data accessibility

All data collected as part of this work are directly presented in the text and figures of the manuscript.

## Highlights

1. DSS alleviated BLM-induced PF in mice.
2. DSS repressed TGF- $\beta$ 1-induced PF in NIH3T3 cells.
3. DSS might be a potential therapeutic drug for PF treatment.

## Statement of ethics

All procedures were approved by the Animal Research Ethics Board of The Affiliated Hospital of Shandong University of Traditional Chinese Medicine and all experiments were performed in accordance with relevant guidelines and regulations.

## References

- [1] Richeldi L, Collard HR, Jones MG. Idiopathic pulmonary fibrosis. *Lancet*. 2017;389(10082):1941–1952.
- [2] Wynn TA. Integrating mechanisms of pulmonary fibrosis. *J Exp Med*. 2011;208(7):1339–1350.
- [3] Raghu G, Weycker D, Edelsberg J, et al. Incidence and prevalence of idiopathic pulmonary fibrosis. *Am J Respir Crit Care Med*. 2006;174(7):810–816.
- [4] Khalil N, O'Connor R. Idiopathic pulmonary fibrosis: current understanding of the pathogenesis and the status of treatment. *Cmaj*. 2004;171(2):153–160.
- [5] Li L, Cai L, Zheng L, et al. Gefitinib inhibits bleomycin-induced pulmonary fibrosis via alleviating the oxidative damage in mice. *Oxid Med Cell Longev*. 2018;2018:8249693.
- [6] Crystal RG, Bitterman PB, Rennard SI, et al. Interstitial lung diseases of unknown cause. Disorders characterized by chronic inflammation of the lower respiratory tract (first of two parts). *N Engl J Med*. 1984;310(3):154–166.
- [7] Munger JS, Huang X, Kawakatsu H, et al. The integrin  $\alpha$ v $\beta$ 6 binds and activates latent TGF $\beta$ 1: a mechanism for regulating pulmonary inflammation and fibrosis. *Cell*. 1999;96(3):319–328.
- [8] Ramos C, Montaña M, García-Alvarez J, et al. Fibroblasts from idiopathic pulmonary fibrosis and normal lungs differ in growth rate, apoptosis, and tissue inhibitor of metalloproteinases expression. *Am J Respir Cell Mol Biol*. 2001;24(5):591–598.
- [9] Kim KK, Kugler MC, Wolters PJ, et al. Alveolar epithelial cell mesenchymal transition develops in vivo during pulmonary fibrosis and is regulated by the extracellular matrix. *Proc Natl Acad Sci U S A*. 2006;103(35):13180–13185.
- [10] Li X, Bi Z, Liu S, et al. Antifibrotic mechanism of cinobufagin in bleomycin-induced pulmonary fibrosis in mice. *Front Pharmacol*. 2019;10:1021.
- [11] Zhang K, Rekhter MD, Gordon D, et al. Myofibroblasts and their role in lung collagen gene expression during

- pulmonary fibrosis. A combined immunohistochemical and in situ hybridization study. *Am J Pathol.* **1994**;145(1):114–125.
- [12] Gabbiani G. The biology of the myofibroblast. *Kidney Int.* **1992**;41(3):530–532.
- [13] Zhang J, Zhang Q, Liu G, et al. Therapeutic potentials and mechanisms of the Chinese traditional medicine Danshensu. *Eur J Pharmacol.* **2019**;864:172710.
- [14] Luo J, Zhang L, Zhang X, et al. Protective effects and active ingredients of *Salvia miltiorrhiza* Bunge extracts on airway responsiveness, inflammation and remodeling in mice with ovalbumin-induced allergic asthma. *Phytomedicine.* **2019**;52:168–177.
- [15] Cao G, Zhu R, Jiang T, et al. Danshensu, a novel indoleamine 2,3-dioxygenase1 inhibitor, exerts anti-hepatic fibrosis effects via inhibition of JAK2-STAT3 signaling. *Phytomedicine.* **2019**;63:153055.
- [16] Lu H, Tian A, Wu J, et al. Danshensu inhibits  $\beta$ -adrenergic receptors-mediated cardiac fibrosis by ROS/p38 MAPK axis. *Biol Pharm Bull.* **2014**;37(6):961–967.
- [17] Ji Y, Wang T, Wei ZF, et al. Paeoniflorin, the main active constituent of *Paeonia lactiflora* roots, attenuates bleomycin-induced pulmonary fibrosis in mice by suppressing the synthesis of type I collagen. *J Ethnopharmacol.* **2013**;149(3):825–832.
- [18] Vu TN, Chen X, Foda HD, et al. Interferon- $\gamma$  enhances the antifibrotic effects of pirfenidone by attenuating IPF lung fibroblast activation and differentiation. *Respir Res.* **2019**;20(1):206.
- [19] Katzenstein AL, Myers JL. Idiopathic pulmonary fibrosis: clinical relevance of pathologic classification. *Am J Respir Crit Care Med.* **1998**;157(4):1301–1315.
- [20] Canestaro WJ, Forrester SH, Raghu G, et al. Drug treatment of idiopathic pulmonary fibrosis: systematic review and network meta-analysis. *Chest.* **2016**;149(3):756–766.
- [21] Galli JA, Pandya A, Vega-Olivo M, et al. Pirfenidone and nintedanib for pulmonary fibrosis in clinical practice: tolerability and adverse drug reactions. *Respirology.* **2017**;22(6):1171–1178.
- [22] Li LC, Kan LD. Traditional Chinese medicine for pulmonary fibrosis therapy: progress and future prospects. *J Ethnopharmacol.* **2017**;198:45–63.
- [23] Jia J, Mo X, Liu J, et al. Mechanism of danshensu-induced inhibition of abnormal epidermal proliferation in psoriasis. *Eur J Pharmacol.* **2020**;868:172881.
- [24] Zhang L, Wu T, Chen JM, et al. Danshensu inhibits acetaldehyde-induced proliferation and activation of hepatic stellate cell-T6. *Zhong Xi Yi Jie He Xue Bao.* **2012**;10: 1155–1161.
- [25] Zhang N, Dong M, Luo Y, et al. Danshensu prevents hypoxic pulmonary hypertension in rats by inhibiting the proliferation of pulmonary artery smooth muscle cells via TGF- $\beta$ -smad3-associated pathway. *Eur J Pharmacol.* **2018**;820:1–7.
- [26] Chen YS, Lee SM, Lin YJ, et al. Effects of danshensu and salvianolic acid B from *Salvia miltiorrhiza* Bunge (Lamiaceae) on cell proliferation and collagen and melanin production. *Molecules.* **2014**;19(2):2029–2041.
- [27] Ji Y, Dou YN, Zhao QW, et al. Paeoniflorin suppresses TGF- $\beta$  mediated epithelial-mesenchymal transition in pulmonary fibrosis through a Smad-dependent pathway. *Acta Pharmacol Sin.* **2016**;37(6):794–804.
- [28] Wang G, Wu H, Liang P, et al. Fus knockdown inhibits the profibrogenic effect of cardiac fibroblasts induced by angiotensin II through targeting Pax3 thereby regulating TGF- $\beta$ 1/Smad pathway. *Bioengineered.* **2021**;12(1):1415–1425.
- [29] Yang Y, Xiao C, Liu K, et al. Silencing of long non-coding INHBA antisense RNA1 suppresses proliferation, migration, and extracellular matrix deposition in human hypertrophic scar fibroblasts via regulating microRNA-141-3p/myeloid cell leukemia 1 axis. *Bioengineered.* **2021**;12(1):1663–1675.
- [30] Li ZM, Xu SW, Liu PQ. *Salvia miltiorrhiza* Burge (Danshen): a golden herbal medicine in cardiovascular therapeutics. *Acta Pharmacol Sin.* **2018**;39:802–824.
- [31] Shao R, Wang FJ, Lyu M, et al. Ability to suppress TGF- $\beta$ -activated myofibroblast differentiation distinguishes the anti-pulmonary fibrosis efficacy of two danshen-containing chinese herbal medicine prescriptions. *Front Pharmacol.* **2019**;10:412.
- [32] Bartram U, Speer CP. The role of transforming growth factor beta in lung development and disease. *Chest.* **2004**;125(2):754–765.
- [33] Kim KK, Sheppard D, Ha C. TGF- $\beta$ 1 signaling and tissue fibrosis. *Cold Spring Harb Perspect Biol.* **2018**;10(4):a022293.
- [34] Ignatz RA, Massagué J. Transforming growth factor-beta stimulates the expression of fibronectin and collagen and their incorporation into the extracellular matrix. *J Biol Chem.* **1986**;261(9):4337–4345.
- [35] Roberts AB, Sporn MB, Assoian RK, et al. Transforming growth factor type beta: rapid induction of fibrosis and angiogenesis in vivo and stimulation of collagen formation in vitro. *Proc Natl Acad Sci U S A.* **1986**;83(12):4167–4171.
- [36] Kulkarni AB, Huh CG, Becker D, et al. Transforming growth factor beta 1 null mutation in mice causes excessive inflammatory response and early death. *Proc Natl Acad Sci U S A.* **1993**;90(2):770–774.
- [37] Shull MM, Ormsby I, Kier AB, et al. Targeted disruption of the mouse transforming growth factor-beta 1 gene results in multifocal inflammatory disease. *Nature.* **1992**;359(6397):693–699.
- [38] Travis MA, Sheppard D. TGF- $\beta$  activation and function in immunity. *Annu Rev Immunol.* **2014**;32(1):51–82.

- [39] Vannella KM, Wynn TA. Mechanisms of organ injury and repair by macrophages. *Annu Rev Physiol.* 2017;79(1):593–617.
- [40] Minutti CM, Knipper JA, Allen JE, et al. Tissue-specific contribution of macrophages to wound healing. *Semin Cell Dev Biol.* 2017;61:3–11.
- [41] Krafts KP. Tissue repair: the hidden drama. *Organogenesis.* 2010;6(4):225–233.
- [42] Thannickal VJ, Lee DY, White ES, et al. Myofibroblast differentiation by transforming growth factor-beta1 is dependent on cell adhesion and integrin signaling via focal adhesion kinase. *J Biol Chem.* 2003;278(14):12384–12389.
- [43] Gauldie J, Sime PJ, Xing Z, et al. Transforming growth factor-beta gene transfer to the lung induces myofibroblast presence and pulmonary fibrosis. *Curr Top Pathol.* 1999;93: 35–45.
- [44] Liu G, Zhang Q, Zhang J, et al. Preventive but non-therapeutic effect of danshensu on hypoxic pulmonary hypertension. *J Int Med Res.* 2020;48(5):300060520914218.
- [45] Qu W, Huang H, Li K, et al. Danshensu-mediated protective effect against hepatic fibrosis induced by carbon tetrachloride in rats. *Pathol Biol.* 2014;62(6):348–353.
- [46] Reagan-Shaw S, Nihal M, Ahmad N. Dose translation from animal to human studies revisited. *FASEB J.* 2008;22(3):659–661.
- [47] Chen H, Chen H, Liang J, et al. TGF- $\beta$ 1/IL-11/MEK/ERK signaling mediates senescence-associated pulmonary fibrosis in a stress-induced premature senescence model of Bmi-1 deficiency. *Exp Mol Med.* 2020;52(1):130–151.
- [48] Galuppo M, Esposito E, Mazzon E, et al. MEK inhibition suppresses the development of lung fibrosis in the bleomycin model. *Naunyn-Schmiedeberg's Arch Pharmacol.* 2011;384(1):21–37.
- [49] Madala SK, Schmidt S, Davidson C, et al. MEK-ERK pathway modulation ameliorates pulmonary fibrosis associated with epidermal growth factor receptor activation. *Am J Respir Cell Mol Biol.* 2012;46(3):380–388.
- [50] Ye T, Xiong D, Chen L, et al. Effect of Danshen on TLR2-triggered inflammation in macrophages. *Phytomedicine.* 2020;70:153228.
- [51] Tang F, Zhou X, Wang L, et al. A novel compound DT-010 protects against doxorubicin-induced cardiotoxicity in zebrafish and H9c2 cells by inhibiting reactive oxygen species-mediated apoptotic and autophagic pathways. *Eur J Pharmacol.* 2018;820:86–96.